Report for IOR project: Calibrating the overburden model with time-lapse data

Authors:

Jan Øystein Bakke, Jarle Haukås and Lars Sønneland

Schlumberger Stavanger Research

Version 1 – August 2014

Table of Contents

Introduction 1
3D geomechanical earth model 1
Top reservoir displacement boundary condition 1
Simulated versus observed time shift 2
Simulated versus observed time strain 3
Boundary condition strain consistency check 4
Mismatch analysis in terms of R-factor 7
Research proposal: Integrated dynamic drilling hazard identification 8
References 8

Introduction

Pressure depletion and water weakening of the chalk reservoir rock leads to reservoir compaction that results in a downwards displacement of the top reservoir interface. The displacement induces an overburden strain that spreads all the way up to the seabed. Due to lateral variations in the vertical displacement, shear forces are introduced, and both compaction and dilation of the overburden rock may occur. The presence of shear forces may lead to reactivation of faults and well collapses, and represents a drilling hazard when placing new wells.

To model overburden stresses and strains, an estimate of the top reservoir displacement is required. For this purpose, there exists a coupled geomechanical model of the reservoir and overburden, including a reservoir chalk model for compaction prediction. However, the reservoir model is uncertain, and the predicted displacements from the current model are not necessarily consistent with the top reservoir displacements derived from time-lapse seismic data.

Instead of relying on a reservoir chalk model, the observed time-lapse displacement of top reservoir is used as a boundary condition for the overburden geomechanical model. This is a novel approach where simulation and observation agree at top reservoir, while an overburden mismatch can be attributed to an imperfect choice of model properties and / or variation in the velocity sensitivity of the overburden rock (the R-factor (Hatchel, 2005)). The mismatch is analyzed in terms of time shift versus simulated displacement and time strain versus simulated strain. The goal is to update the overburden model to reduce the mismatch. We note that leaving out the mechanical complexities of the reservoir from the model greatly reduces simulation run times, so that quick scenario screening becomes feasible.

In the following, the boundary condition approach is presented in more detail. Comparisons of simulated and observed time shift and time strain are shown, and the mismatch between simulation and observation is discussed. In particular, the R-factor is estimated that would be required to explain the difference between simulated strain and observed time strain. Finally, an evaluation is given focusing on whether reported well collapses agree with regions of shear strain in the simulation model.

3D geomechanical earth model

The geometry of the 3D geomechanical earth model is based on horizons from seismic data acquired in 2006, subdivided into layers for increased vertical resolution. The model is populated with anisotropic material properties from 1D MEMs (well logs) and faults extracted from seismic data. The initial stresses and strains are established by gravity/pore pressure initialization taking into account the density of the rock, the pore pressure gradient, stress ratios and dominant stress direction, material properties and fault/fracture properties. The initialization includes reservoir, overburden, sideburden and underburden.

Top reservoir displacement boundary condition

Given the initial stress state of the overburden, vertical displacement increments can be added at top reservoir to simulate the associated stress and strain change. The seabed boundary is treated as a free surface, while the displacement increments at the lateral model boundaries are set to zero, as shown in Figure 1. The top reservoir displacement boundary condition is derived from the time-shift at top reservoir, as described in the following.

Time shifts can be calculated by e.g., correlation analysis for any pair of time-lapse data. The time shift is a function of seabed subsidence and accumulated overburden strain and velocity change,

$$\delta t = \frac{2}{v_w}\delta z_{SB} + \sum_k \frac{2(1+R_k)}{v_k}\Delta z_k = \frac{2}{v_w}\delta z_{SB} + \frac{2(1+\mathrm{R})}{\mathrm{v}}(\delta z - \delta z_{SB}). \quad (1)$$

Here δz denotes interface displacement, Δz denotes thickness change, v is velocity and R is the so-called R-factor. Subscript k indicates an overburden layer / interval; subscript w is for water velocity, while the SB subscript is used for seabed subsidence. The R-factor, which is generally both lithology and stress dependent, estimates the effect of velocity change relative to the effect of the actual displacement. Since the R-factor of the individual overburden layers is not known, an average representative value is used. Previous studies suggest an average value of R = 5 for the bulk response of the overburden in a nearby field (Hatchell, 2005). We have used this R-value and an average velocity of around 2000 m/s (consistent with the overburden interval velocity model).

By rearranging terms in (1) we find that the displacement at top reservoir can be expressed as:

$$\delta z_{TR} = \frac{\mathrm{v}}{2(1+R)}\delta t_{TR} + \left(1 - \frac{v}{v_w(1+R)}\right)\delta z_{SB} = \frac{\mathrm{v}}{2(1+R)}\delta t_{TR} + \left(\frac{\mathrm{v}_w}{2} - \frac{v}{2(1+R)}\right)\delta t_{SB}. \quad (2)$$

The time-shift at top reservoir is available from the time-lapse data. For the seabed term, bathymetry data, an assumed ratio between reservoir and seabed subsidence or the time-shift at seabed is required. For small time-lapse periods, the seabed term has less impact. The estimate from (2) is input to the geomechanical simulator as a displacement increment to produce changes in stresses and strains.

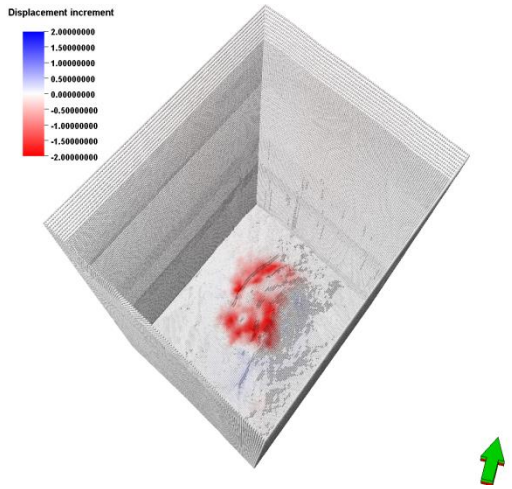

Figure 1: Displacement increment applied to top reservoir and sides (point set display with

Simulated versus observed time shift

Simulated time shift is obtained from simulated displacement by using (1). The simulated time shift at top reservoir honors the observed time shift if the same R-factor and average velocity is used in the

conversion. Hence, the mismatch between simulated and observed data is only associated with how the displacements spread and decay into the overburden. Figure 2 and Figure 3 show comparisons between simulated and observed time shifts between 2010 and 2012, and between 1988 and 1999. We note that the mismatch in the upper half of the overburden is due to the fact that the observed time shift is contaminated by noise. Similar results have been obtained for time-lapse pairs involving surveys in 2003, 2006 and 2008. Overall, the observed and simulated time-shifts are quite similar. Quantitative analysis of the mismatch between simulation results and the time-lapse data is presented later.

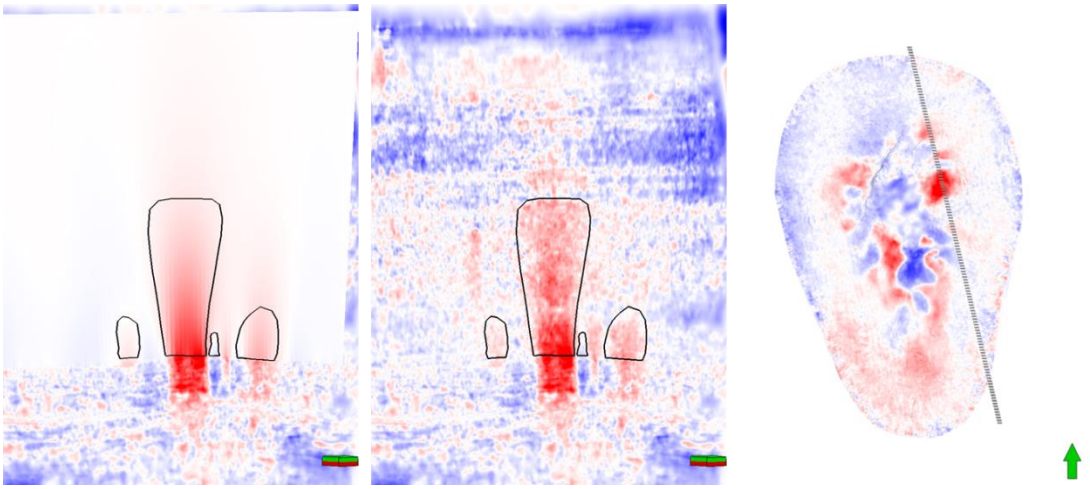

Figure 2: Simulated time shift (left) versus observed time shift (middle) for the LoFS1-LoFS4 time period for an intersection crossing a subsidence anomaly in the top reservoir subsidence map (right). Black polygons are drawn to make it easier to compare.

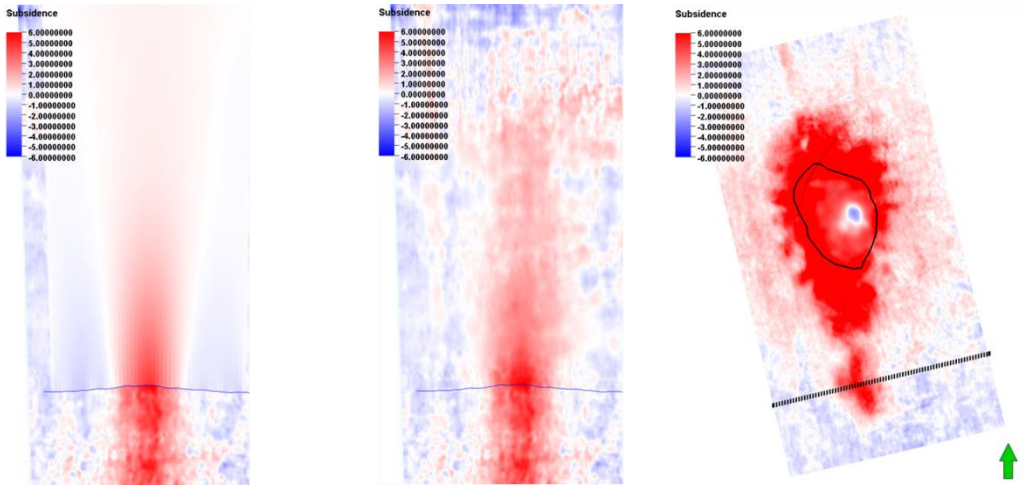

Figure 3: Simulated time shift (left) versus observed time shift (middle) for the 1988-1999 time period for an intersection crossing a subsidence anomaly in the top reservoir subsidence map (right). The black polygon indicates the seismically obscured area.

Simulated versus observed time strain

For an overburden layer *k*, simulated time strain is related to simulated strain by

$$TS_k = 2(1 + R_k)\varepsilon_{zz,k}. \quad (3)$$

Over the corresponding time interval, t_n to t_m, the observed time strain is estimated from time shift:

$$\left(\frac{d(\delta t)}{dt}\right)_k \approx \frac{\delta t_n - \delta t_m}{t_n - t_m}. \quad (4)$$

When estimated over short intervals, the time strain estimate (4) tends to oscillate between positive and negative values, due to noise in the time shift estimate. To avoid such unphysical oscillations, we average the time shift over a larger interval prior to estimating the time strain, as illustrated in Figure 4. We note that without the averaging procedure, a quantitative comparison between observed and simulated strain would be very difficult, as the lower plots in Figure 4 indicate.

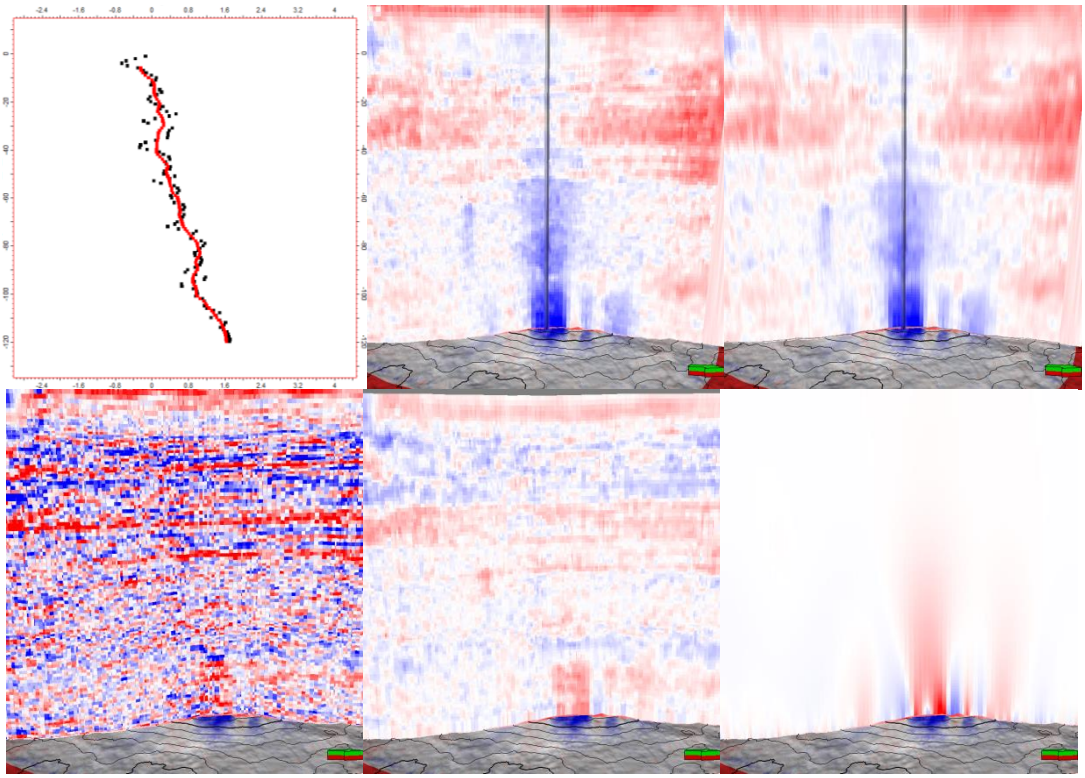

Figure 4: Upper left: Original time shift (black) and averaged time shift (red) versus grid layer number along vertical grid column. Upper middle: original time shift with reference grid column shown. Upper right: averaged time shift with reference grid column shown. Lower left: time strain from original time shift. Lower middle: time strain from averaged time shift. Lower left: simulated time strain from simulated strain with R = 5. All time-lapse data are from the LoFS1-LoFS4 time period.

Boundary condition strain consistency check

The displacement of top reservoir induces strain that spreads into the overburden. Even if the top reservoir displacement is strictly downwards, both overburden compaction and dilation can be observed and simulated, as shown in Figure 5.

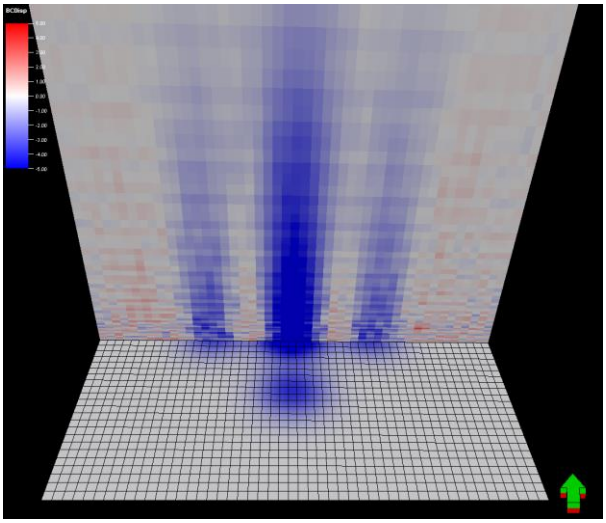

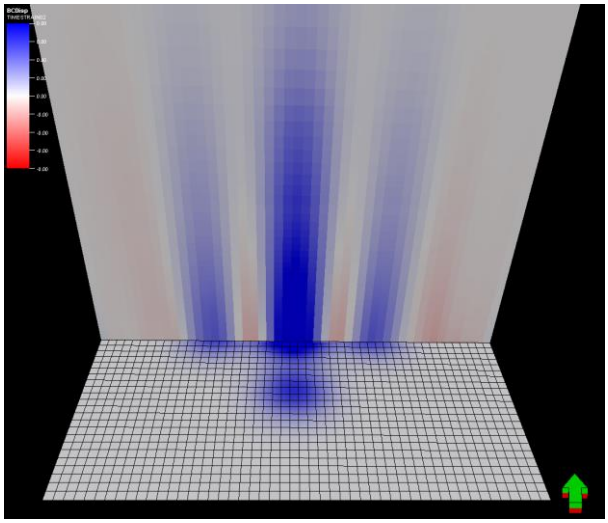

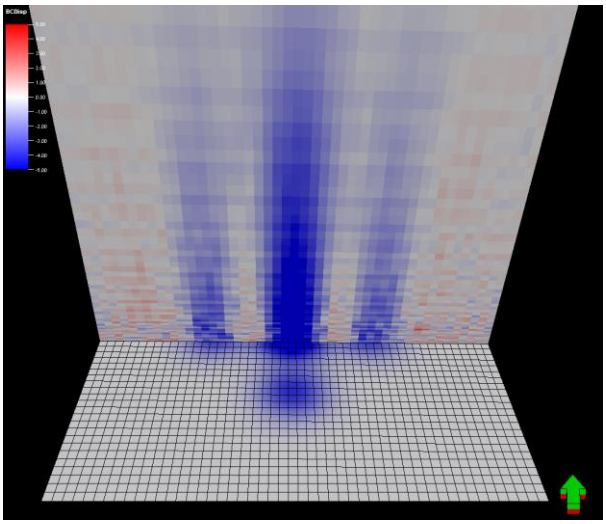

Figure 5

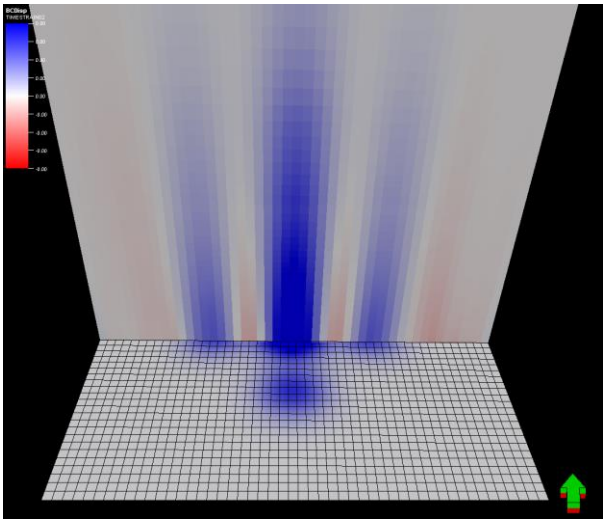

Figure 5: Intersection of observed time-strain (left) and simulated vertical strain (right). Top reservoir subsidence shown as attribute on top reservoir map (both figures). The top reservoir displacement is shown on the surface. It is strictly

downwards. Both overburden compaction (red) and dilation (blue) is present although the top reservoir displacement is strictly downwards.

Further analysis shows that overburden dilation originates from local maxima in the top reservoir displacement, while compaction originates from local minima in the top reservoir displacement. The principle is illustrated in Figure 6.

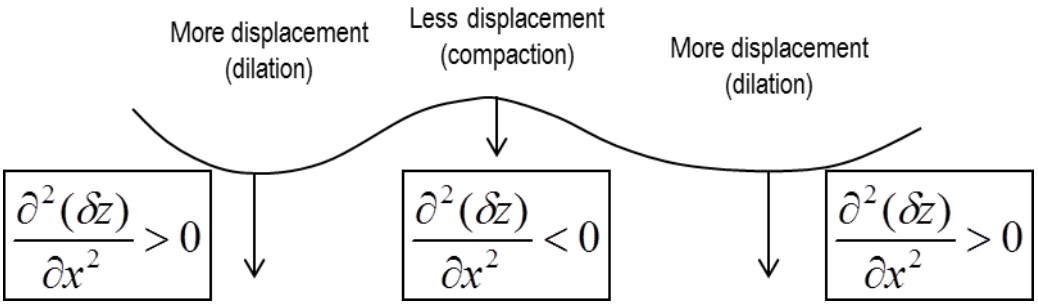

Figure 6: Sketch of relationship between differential slope of displacement at an interface and compaction versus dilation in the region above.

Cross plots of simulation results as shown in Figure 7 indicate that the vertical strain is approximately proportional to the differential slope of the vertical displacement:

$$\varepsilon_{zz} = -\beta\left(\frac{\partial^2(\delta z)}{\partial x^2} + \frac{\partial^2(\delta z)}{\partial y^2}\right). \qquad (5)$$

The factor β seems fairly constant in the region close to top reservoir. For shallower regions, β increases (not shown here), but the strain and the differential slope of the displacement remain approximately proportional for a given overburden layer.

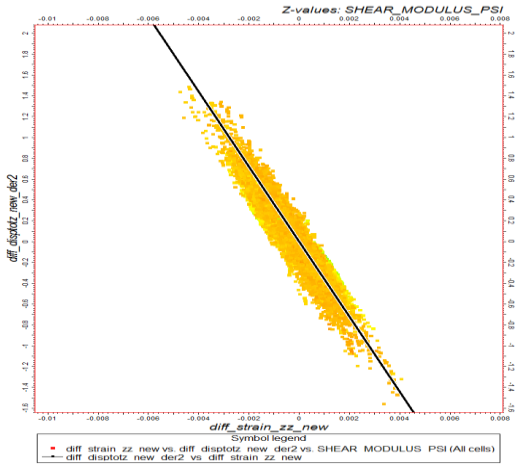

Figure 7: Cross plot of second derivatives of vertical displacement versus vertical strain (from simulation results).

We note that the relationship (5) is similar to a relationship known from simple plate theory and from studies of subsidence in coal mining. It can be derived (Bise 2013) that horizontal strains are related to the differential slope of displacement by

$$\varepsilon = B\frac{\partial^2(\delta z)}{\partial x^2} \quad (6)$$

Here B is a function of the distance to the neutral axis of the plate / the mine seam, and the bending angle. However, to obtain Eqn. (5), an additional relationship between horizontal and vertical strains is required.

Eqn. (5) provides a simple consistency check between the displacement boundary condition and the resulting strain. By taking the second derivatives of the displacement boundary condition at top reservoir and using Eqn. (5), we have an estimate of the strain around top reservoir, and can identify the origin of overburden compaction zones (negative differential slope of displacement at top reservoir) and overburden dilation zones (positive differential slope). This estimate should agree with the observed time strain around top reservoir, at least in terms of sign.

In regions where the simulated strain does not match the estimated time-strain around top reservoir, further investigation is necessary. If the time-lapse data around top reservoir are reliable, the mismatch implies that the boundary condition should be modified. This can be done by updating the seabed term and/or the overburden term (R-factor and velocity). We have also tested an approach where Eqn. (5) is solved with respect to the displacement δz in regions where the simulated strain does not match the sign of the observed time strain. The resulting changes in displacement from the initial estimate may be attributed to lateral variations in the R-factor, in the overburden velocity or in the seabed term.

Mismatch analysis in terms of R-factor

A difference between simulated strain and observed time-strain may be used to update the overburden model in several different ways:

- The assumed velocity sensitivity of the overburden layers (R-factor model) could be updated, so that the simulated strain converted to time strain becomes more similar to the observed time strain.
- The material parameters could be updated so that the simulated strain better matches the observed time strain.

In general it may be difficult to identify whether the mismatch is related to the R-factor model or the material model. In any case, a quantification of the mismatch is necessary for the interpretation.

If we assume that the difference can be explained by the R-factor only, we can combine equations (3) and (4) to derive the estimate

$$R_k = \frac{\left(\frac{\mathrm{d}(\delta \mathrm{t})}{dt}\right)_k}{2\varepsilon_{zz,k}} - 1. \quad (7)$$

According to Janssen et al. (2007), R-factors from 1 to 10 are reasonable. R values from the estimate (7) that exceeds the expected value range may indicate anomalies in the overburden model, possibly including fracture zones. Regions where the estimated R-factor is negative imply a more profound mismatch, where the simulation suggests compaction while the observation shows dilation and vice

versa. In regions where a reasonable and positive R-factor can be found, it should be investigated whether the R-factor estimate is sensitive to time-lapse changes between time-lapses, or if it is an inherent material property that is consistent between the different time-lapses.

Research proposal: Integrated dynamic drilling hazard identification

Schlumberger Stavanger Research is in collaboration with an oil company and the University of Bergen working on a research proposal on reservoir monitoring. The project will incorporate passive seismic measurements from a permanent reservoir monitoring system as well as frequent time-lapse seismic in a workflow for describing high fidelity drilling hazards in the overburden and in the reservoir.

The use of passive seismic monitoring is also of interest in a IOR-scenario where fracturing caused by increased injection pressure / water weakening can be used to track fluid and pressure fronts. This information can be incorporated into history matching schemes.

References

Bise, C.J. Modern American Coal Mining: Methods and Applications. Society for Mining, Metallurgy, and Exploration (SME), 2013.

Hatchell, P.J.; Bourne, S.J. Measuring reservoir compaction using time-lapse timeshifts, SEG Annual meeting, 2005

Janssen, A.L., Smith, B.A., Byerley, G.W. Measuring Seismic Velocity Sensitivity to Production-Induced Strain at the Ekofisk Field. Offshore Technology Conference, 2007.